



**UNIVERSITATEA MARITIMĂ DIN CONSTANȚA
ȘCOALA DOCTORALĂ DE INGINERIE MECANICĂ ȘI MECATRONICĂ**

TEZĂ DE DOCTORAT

**STUDII DE OPTIMIZARE A CÂMPURILOR DE
CURGERE REACTANȚI DIN CADRUL PILELOR DE
COMBUSTIE CU MEMBRANĂ SCHIMBĂTOARE
DE PROTONI (PEMFC)**

**OPTIMISATION STUDIES OF THE REACTANT FLOW
FIELDS FROM PROTON EXCHANGE MEMBRANE
FUEL CELLS (PEMFC)**

REZUMAT în limba engleză

Autor: Ing. Viorel IONESCU

Conducător de doctorat: Prof.Dr.Ing. Nicolae BUZBUCHI

CONSTANȚA

2019

SUMMARY OF THE DOCTORAL THESIS

List of notations.....	3
Index of figures.....	7
Index of tables.....	13
Thanks.....	15
Chapter 1. Introduction	
Objectives of the doctoral thesis.....	16
Structure of the doctoral thesis.....	17
Chapter 2. Current research on the optimization of bipolar plates in PEMFCs	
2.1. Fundamental aspects of PEMFC.....	19
2.1.1. Fuel cells. Short history.....	19
2.1.2. Overview of PEMFC technology and operation.....	22
2.1.3. Water management in the PEMFC cell.....	27
2.1.4. Industrial Applications of PEMFC.....	29
2.2. Experimental studies and modeling of flow fields in PEMFC.....	39
2.2.1. Brief review of PEMFC numerical models.....	39
2.2.2. Current studies on the influence of the reaction gas flow geometry on PEMFC performance.....	41
2.2.3. Preliminary numerical analysis using 2D and 3D models implemented through Finite Element Method (FEM) to optimize reagent flow channels.....	44
Chapter 3. Using the Energy and Exergy Concept to specify the Efficiency of a PEMFC	
3.1. Energy analysis of the fuel cell.....	58
3.2. Exergy analysis of the fuel cell.....	61
Chapter 4. Description of mathematical models used to evaluate PEMFC flow field performance	
4.1. Semi-empirical mathematical model for the evaluation of voltage losses according to operating parameters.....	65
4.1.1. Control of gas pressure in the PEMFC system.....	65
4.1.2. Assessment of net outflow in the combustion cell.....	67
4.1.3. Effect of pressure on open circuit voltage (OCV) and on proton membrane resistance in PEMFC.....	69
4.2. Elements of Fluid Mechanics in Mathematical Analysis of Reaction Fields with Coil Channels.....	73
4.2.1. Analysis of reactant gas flow channels.....	73
4.2.2. Design of the three PEMFC gas channel flow fields.....	79
4.2.3. The relative influence of convection within the flow fields.....	84
4.3. Equations of 3D numerical model for CFD analysis of transport phenomena in PEMFC.....	93
Chapter 5. Numerical modeling of the proton exchange membrane fuel cell	
5.1. Numerical FEM analysis of the PEMFC unit cell.....	97
5.1.1. 3D modeling elements in Comsol Multiphysics.....	97
5.1.2. Equations of government.....	100
5.1.3. Numerical analysis of PEMFC reactance distribution with three different flow fields...	107

5.2. Study of local transport phenomena for a two-channel PEMFC system in the form of a serpentine.....	109
5.2.1. Elements for calculating parameters specific to inter-channel convection.....	109
5.2.2. 3D numerical model for the study of the transport of the reaction mass following the change in the geometric dimensions of the flow channel.....	115
5.3. Influence of pressure in the PEMFC system on pile voltage losses according to semi-empirical model.....	121
5.3.1. The effect of the outlet pressure on the partial pressure of the reaction gas.....	121
5.3.2. Calculation of different voltage losses at different output pressures.....	122
Chapter 6. Energy, Exergy Analysis and Current-Voltage stability for PEMFC with three different reactant gas flow fields	
6.1. Description of the PEMFC experimental test system.....	125
6.1.1. Presentation of the control system inside the PEMFC station.....	125
6.1.2. Experimental test assembly.....	129
6.2. Study of output voltage variations and voltage stability at constant load.....	136
6.2.1. Investigating the performance of the three flow fields at two different exit pressures....	136
6.2.2. Effect of the MEA on fuel cell stability at high current densities.....	140
6.3. Evaluation of energy and exergetic efficiency under the influence of output pressure.....	143
6.3.1. Energy efficiency study.....	143
6.3.2. Study of exergy efficiency.....	144
6.4. Influence of Electrode Membrane Assembly (MEA) on PEMFC efficiency.....	147
6.4.1. Comparative analysis of polarization curves and energy efficiency.....	147
6.4.2. Comparative study of the exergetic efficiency of the combustion cell with different MEAs.....	149
Chapter 7. Experimental validation of semi-empirical model and FEM numerical model	
7.1. Validation of the semi-empirical model based on PEMFC current-voltage experimental characteristic with optimized flow field.....	152
7.2. Validation of the 3D numerical model using PEMFC's current-voltage experimental curves.....	153
Chapter 8. Personal Contributions, Conclusions and Future Research Directions	
8.1. Conclusions.....	158
8.2. Personal contributions.....	162
8.3. Future research directions.....	163
Annexes	
Appendix 1: Dissemination of results - papers elaborated by the author.....	164
Appendix 2: BEKKTECH water temperature stability test with thermocouple.....	165
Appendix 3: Catalog data - PEMFC experimental test system components.....	167
Bibliography	177

PhD THESIS SUMMARY

The present paper extends to 183 pages and includes 115 figures, 25 tables, 3 annexes and 170 bibliographic references.

Keywords: bipolar plate, serpentine channels, pressure drop, backpressure, binary diffusion, bypass convection, channel width, channel rib, concentration gradient, molar fraction, current density, polarisation curve, ohmic losses, stoichiometric ratio, energy efficiency, exergy, thermodynamic irreversibility.

1. INTRODUCTION

Proton Exchange Membrane Fuel Cells (PEMFC) became nowadays very popular for transportation applications in Fuel Cell Hybrid Electric Vehicles (FCHEV) due to a low operation temperatures, high energy densities and high fuel efficiencies, fuel cell stack being hybridized here with a supercapacitor or high power battery in order to improve its slow dynamics and peak power supplying capability. PEM fuel cell stacks provide an easier maintenance with reduced costs due to a low number of moving parts in the entire energy system, produce zero harmful emissions (only heat and water as waste products), offer high quality DC power and have high degree of reliability.

Bipolar plates, as one of the main components of a Proton Exchange Membrane Fuel Cell (PEMFC) system, offer a path for a uniform distribution of reactant gases via flow channels, dissipate heat from reaction sites, prevent leakage of gases and offer the electrical connection between multiple cells in a stack.

Numerical research studies related to optimization of bipolar plate flow fields in PEMFC, developed in order to increase the fuel cell efficiency have been focused on the channel geometry involving width " a ", height " b " and inter-channel distance " w " – rib width (distance between two adjacent channels). The most efficient type of reactant flow field used for bipolar plates of a PEM fuel cell was reported to be the field with channels oriented in serpentine configuration. A number of advantages and disadvantages have been reported in the literature regarding the effect of the ratio $w/a > 1$ on the performance of the PEMFC system. As the main advantages, it was distinguished: an enhanced mechanical support for membrane and Gas Diffusion Layer (GDL), higher water content in the membrane, improved ion conductivity of the membrane, improved heat transfer from membrane to GDL, uniform distribution of the current density and temperature across the membrane and improved performance at high current densities. The most important drawbacks reported were: a less efficient removal of water as a reaction product through GDL, higher pressure drop across the flow field, a reduced contact area between reactants and GDL and higher overall voltage losses.

Increasing levels of backpressure in a PEM fuel cell system resulted in increases in the exchange current densities of the electrochemical reactions, with the increase in the reactant partial pressures. Backpressure can help to increase the fuel cell performance by increasing the oxygen and hydrogen diffusion to the active sites of the catalyst layer (CL). Backpressure valve at cathode for a hybrid PEM fuel cell vehicle represent one of the main control parameters for the fuel cell stack performance.

The exergy analysis offer precise system efficiency results by considering the thermodynamic losses within the system and passing in this way the limitations of energy analysis. It is a useful tool for furthering the goal of more efficient energy use, as it enables the determination of the location, type and true magnitude of energy wastes and losses in a system.

Exergy analysis is taken in consideration also for the fuel cell cost assessment, the cost of produced electricity being determined starting from the exergy value.

Starting from all those reported positive/negative effects of the bipolar plate flow channel width/rib width ratios around the value of 1 on the PEM fuel cell performance, in this study it was experimentally investigated the voltage stability at constant load, energy efficiency, exergy efficiency and thermodynamic irreversibility for the fuel cell having three different bipolar plate assemblies with single serpentine flow field channels of different dimensions, using a PEMFC test station working at two different operating backpressures for anode and cathode.

2.SUMMARY OF CHAPTER 2

Numerical 2D modeling studies using Comsol Multiphysics software based on Finite Element Method (FEM) for the PEMFC unit cell have shown that reducing the inter-channel w distance from 1.5 mm to 0.7 mm leads to an improvement in the by-pass convection for oxygen to the cathode, beneficial for a more efficient removal of liquid water from the fuel cell. The local Gas Diffusion Layer/ Catalyst Layer (GDL / CL) current density profile showed the highest values across the cathode input channel of the 2D PEMFC cell model having $a/w = 0.93$ ratio due to the lowest ohmic losses caused by the GDL resistance and the most efficient transfer of oxygen through GDL to CL via the dominant binary diffusion mechanism. It has also been shown by numerical modeling that the hydrogen consumption in the electrochemical reaction at the anode is more uniform across the inter-channel region of the model with $a/w = 0.93$.

I have oriented other 2D numerical modeling studies of the PEMFC unit cell to investigate the influence of the thickness of the Nafion PEM proton membrane proton on the performance of the fuel cell. I considered models with three different thicknesses of Nafion 212 membrane (with a protonic conductivity of 9 S/m at 120°C and 70% RH), i.e. 50 μm , 100 μm and 200 μm . The results of the simulation showed that the 50 μm membrane model had the highest humidity level at the GDL-PEM interface, the highest distribution of the current density at the CL, the smallest ohmic losses produced by the membrane and the lowest superpotential activation of the O_2 reaction at the cathode.

The 3D numerical simulations of the PEMFC unit cell showed the most constant consumption of O_2 at CL across the full length of a flow channel for the model with ration $a/w = 1.2$ (with $a = 1.1$ mm). In all the simulations and experimental tests, the channel height was considered to be 1 mm.

3. SUMMARY OF CHAPTER 3

The *energetic efficiency of the combustion cell* η_{FC} can be determined as: the ratio between the net output power W_{gross} and the rate of hydrogen usage m_{H_2} in accordance with the following relationship:

$$\eta_{FC} = \frac{W_{gross}}{m_{H_2} \cdot LHV_{H_2}} \quad (1)$$

were power $W_{gross} = V_{cell} \cdot I$ (W) is calculated for a current level I (A) considered. LHV_{H_2} represents the „Lower Heating Value” coefficient, having the value of 120.1 MJ/Kg.

The output current is correlated with the H_2 usage rate in accordance with the relation:

$$m_{H_2} = \frac{I}{2F} \times M_{H_2} \text{ (Kg / s)} \quad (2)$$

were M_{H_2} represent hydrogen molar mass, having the value of 2.016×10^{-3} Kg/mol and F is the Faradays constant with the value of 96485.33 A·s/mol.

After a correlation of relations (1) and (2) we obtain a simplified expression for energetic efficiency:

$$\eta_{FC} = \frac{2V_{cell} F}{M_{H_2} \cdot LHV_{H_2}} \quad (3)$$

The exergetic efficiency of the PEMFC system is expressed here as the ratio between the generated electric power $W_{net} = I_{cell} \cdot V_{cell}$ and exergy differences of reactants and products:

$$\eta_{exergy} = \frac{W_{net}}{(Ex_{air,R} + Ex_{H_2,R}) - (Ex_{air,P} + Ex_{H_2O,P})} \quad (4)$$

where Ex (kJ) represents the total exergy of species and subscript R and P represent the reactant and products, respectively.

The total exergy transfer of air and hydrogen streams in PEM fuel cell is written as the sum of the specific physical (ex^{ph}) and chemical (ex^{ch}) exergies, the kinetic and potential exergies being neglected here:

$$Ex = \dot{m}(ex^{ph} + ex^{ch}) \quad (5)$$

with \dot{m} - mass flow rates (Kg/s) of reactant and product species.

For an ideal gas, the physical exergy can be expressed as a function of specific heat at constant pressure c_p and specific heat constant ratio k :

$$ex^{ph} = c_p T_0 \left[\frac{T}{T_0} - 1 - \ln \left(\frac{T}{T_0} \right) + \ln \left(\frac{P}{P_0} \right)^{\left(\frac{k-1}{k} \right)} \right] \quad (6)$$

with the restricted dead state defined by $P_0 = 1$ atm and $T_0 = 298$ K.

Here, the pressure P of humidified gases crossing the combustion cell (from entry to exit) has been considered constant during the test period and estimated in the form of an average value[19], knowing the water vapour saturation pressure of 38.33 kPa and input pressure of the system at anode and cathode: 300 kPa and 200 kPa, respectively in the case of Experiment no. 1.

So, in the case of Experiment no.1, for the test no. 1 performed at a backpressure $P_{b1}=70$ kPa, $P_{1air} = P_{1H_2O} = 1.52$ atm(at cathode) and $P_{1H_2} = 2.015$ atm(at anode). For the test no. 2 at $P_{b2}=30$ kPa, $P_{2air} = P_{2H_2O} = 1.32$ atm and $P_{2H_2} = 1.82$ atm.

The values of the chemical exergies for both of reactants and products in PEM fuel cell are presented in Table 1. Physical properties of the exergy species at the operating conditions of PEMFC system are presented in Table 2.

TABLE I
CHEMICAL EXERGY OF THE REACTANTS AND PRODUCTS OF A PEM FUEL CELL SYSTEM

Chemical exergy, ex^{ch} (kJ/kg)				
Reactant/Product	Reactant air	Reactant H ₂	Product H ₂ O	Product air
BEKKTECH BT-552 system	0	159138	2.5	8.58

TABLE II
PHYSICAL PROPERTIES OF EXERGY SPECIES AT STANDARD OPERATING CONDITIONS

Species	Cp(kJ/Kg·K)	k
H ₂	14.3	1.41
Dry air	1.005	1.40
H ₂ O(vapour)	1.89	1.89

In consequence, the total exergy of reactants and products (expressed in kW) are obtained with relations:

$$Ex_{air,R} = \dot{m}_{air,R} ex_{air,R} = \dot{m}_{air,R} (ex^{ph} + ex^{ch})_{air,R} \quad (7)$$

$$Ex_{H_2,R} = \dot{m}_{H_2,R} ex_{H_2,R} = \dot{m}_{H_2,R} (ex^{ph} + ex^{ch})_{H_2,R} \quad (8)$$

$$Ex_{air,P} = \dot{m}_{air,P} ex_{air,P} = \dot{m}_{air,P} (ex^{ph} + ex^{ch})_{air,P} \quad (9)$$

$$Ex_{H_2O,P} = \dot{m}_{H_2O,P} ex_{H_2O,P} = \dot{m}_{H_2O,P} (ex^{ph} + ex^{ch})_{H_2O,P} \quad (10)$$

The calculated values for the sum between physical and chemical exergies are presented in Table 3 for the two different backpressures considered in experimental testing.

TABLE III
THE SUM OF PHYSICAL AND CHEMICAL EXERGY FOR REACTANTS
AND PRODUCTS

Backpressures	$ex_{air,R}$ (kJ/Kg)	$ex_{air,P}$ (kJ/Kg)	$ex_{H_2,R}$ (kJ/Kg)	$ex_{H_2O,R}$ (kJ/Kg)
30kPa	216.86	225.44	162944.68	410.32
70kPa	242.88	251.46	163114.46	459.26

Thermodynamic irreversibility of the electrochemical processes in the fuel cell I_{IR} is expressed as the difference between the reversible work and useful work. Reversible work is the maximum amount of work obtained from a process. Irreversibility represents the amount of exergy that is “destroyed”, the “lost opportunity” to perform work and when $I_{FC} = 0$, no entropy is generated.

Thermodynamic irreversibility can be written as:

$$I_{IR} = \sum Ex_{heat} + \sum Ex_{mass,in} - \sum Ex_{mass,out} - \sum Ex_{work} \quad (11)$$

were exergy due to heat loss can be estimated with the expression:

$$\sum Ex_{heat} = r_{HL} \times \left(\frac{\Delta H_{g,T}}{2F} - V_{cell} \right) \times I_{cell} \quad (12)$$

with heat loss ratio $r_{HL} = 0.2$.

The enthalpy of water formation in gaseous phase $\Delta H_{g,T}$ is calculated with relation:

$$\Delta H_{g,T} = \Delta H_l^f - \Delta H_T^{vap} \quad (13)$$

where the enthalpy of water formation in liquid phase, $\Delta H_l^f = 285830$ J and the heat of vaporization of water, ΔH_T^{vap} , is evaluated from the following equation:

$$\Delta H_T^{vap} = 3.6985 \times 10^{-4} T_{FC}^3 - 0.4834 T_{FC}^2 - 152.4258 T_{FC} + 68260.5789 \quad (14)$$

with fuel cell operating temperature $T_{FC} = 353$ K.

$$\sum Ex_{mass,in} = Ex_{H_2,R} + Ex_{air,R} \quad (15)$$

$$\sum Ex_{mass,out} = Ex_{H_2,O,P} + Ex_{air,P} \quad (16)$$

and exergy due to the work performed by the cell:

$$\sum Ex_{work} = W_{net} \quad (17)$$

4. SUMMARY OF CHAPTER 4

It was evaluated here first the influence of cathode backpressure (of 30 kPa and 70 kPa) considered in the two PEMFC experiments on the voltage losses induced by the mixed reaction O₂ / Pt and the "crossover" effect of H₂ on the open circuit voltage OCV for the three models of reactant flow fields and the ionic resistance of the PF membrane type Nafion 212 operating at 80 °C and 80% RH. I found that the voltage drops on the fuel cell OCV having the M3 flow field model were 35.2 mV and 19.2 mV respectively, 21% and 47% higher than in the case of M1 model. The ionic resistance of the membrane was slightly decreased by 2.7-3% at high current densities of 0.7-1 A / cm for the backpressure of 70 kPa.

It was described next the design procedure for the three single-channel serpentine channel flow fields tested in the PEMFC assembly, starting with the selection of the two types of MEA assembly with protonic membrane of Nafion 117 and Nafion 212, then it was calculated the length of the flow field having 15 channels and 14 serpentine, along with calculation of the total length of predefined channels characterized by different "a" and "w" values. Thus, the M1 field pattern had the following lengths of the channel lengths and the inter-channel spacing: a = 0.9 mm and w = 0.9 mm, M2 with a = 0.75 mm and w = 0.9 mm and M3, respectively with a = 0.78 mm and w = 0.82 mm. A series of fluid flow parameters for the three field models, such as Reynolds *Re* number, pressure drop across the entire 15-channel system and pressure losses due to the presence of serpentine have been evaluated at volumetric air flow rates of 600 sccm and 800 sccm at cathode, as it was considered in Experiments no. 1 and no. 2. The M3 model showed the highest *Re* value and intermediate pressure drops along the length *L* of the channel system

with a pressure loss ratio of only 0.28%, respectively 0.24% from the total pressure drop along the flow field.

5. SUMMARY OF CHAPTER 5

The 3D numerical analysis of the distribution of the reactants along the flow channel and the GDL layer in the PEMFC unit cell showed for the M3 model the highest level of the hydrogen mass fraction along the length of the GDL and a minimum gradient of this fraction across the unit cell cross-section at the output at a potential of 0.6 V and backpressure of 70 kPa(see fig.1). It has also been recorded for this simulated model more efficient oxygen consumption across the length of the flow channel (see fig. 2).

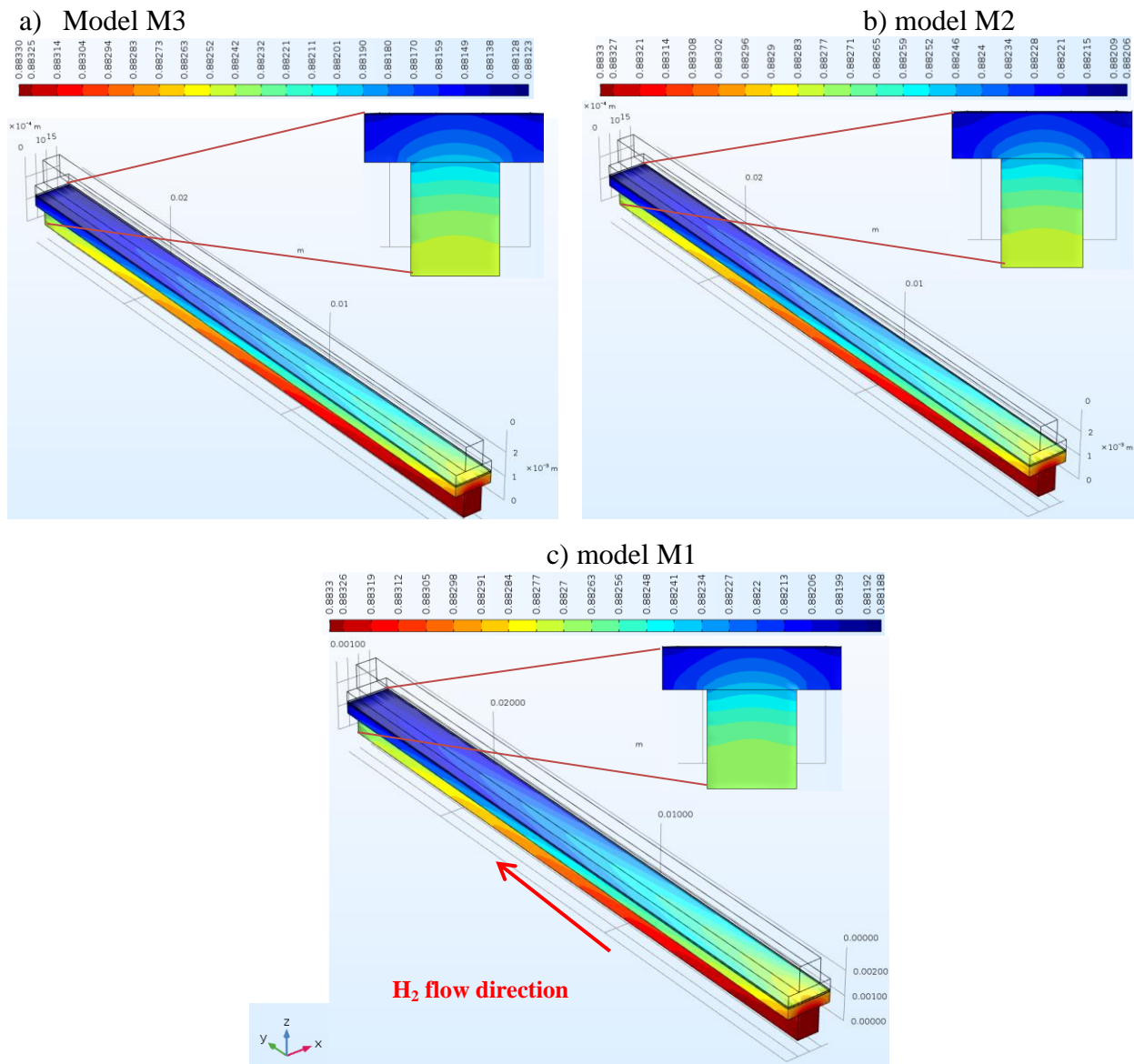


Fig. 1. The distribution of the H₂ mass fraction along the anodic GDL/ flow channel in the xyz plane for a cell operating voltage of 0.6 V at Pb, a = Pb, c = 70 kPa

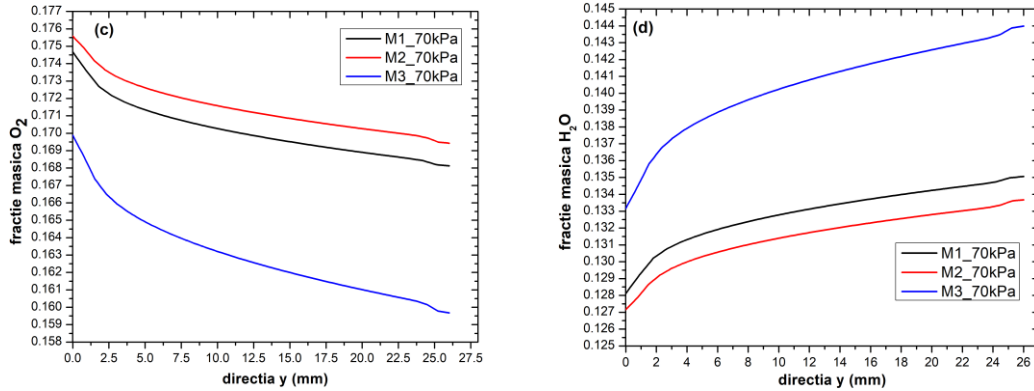


Fig. 2. The variation of the oxygen and water vapor mass fractions at the cathodic GDL-CL interface along the flow direction for the three models M1-M3 at 0.6 V and a backpressure of 70kPa

A semi-empirical mathematical model validated by 3D numerical modeling was used here to evaluate the proportion of the "by-pass" inter-channel convection for a PEMFC model consisting of two channels and a serpentine, adapted for the three flow field models M1-M3. Peclet's number, which has here the role of global inter-channel convection evaluation for air flow at cathode, had the highest values for the M3 model, being about 8% higher than the M2 model over the first half of the active channel flow length. This optimized M3 model showed a convective flow rate of about 16% over the GDL in the region adjacent to the serpentine inside the flow field. The remaining 84% of the flow was associated with the dominant binary diffusion mechanism.

From the numerical simulations of reactant gas transport phenomena at flow channel/GDL interface in the case of the two-channel and a serpentine model of PEMFC unit cell, a more uniform distribution of the current density and flow velocity was observed for M3 model working at a potential of 0.6 V and backpressure of 70 kPa. This optimized model also showed the highest distribution of convective O₂ flux along the CL region.

6. SUMMARY OF CHAPTER 6

Fuel cell performance at different backpressures was measured using a BEKKTECH BT-552 PEMFC test station (based on a single PEM fuel cell unit) in the laboratory of Fuel Cell and Hydrogen Storage, 3Nano-SAE Research Center, Bucharest. The experimental set-up presented in fig. 1 consists of primary components, i.e., Agilent 6060 B 300W electronic load, two MKS RS-485 mass flow controllers, inlet pressure gauges for H₂, N₂ and air, outlet pressure gauges for H₂ and air, two heated/insulated gas lines, H₂/N₂/air tubes with various on/off valves, temperature controllers and two manually controlled back pressure regulators. The components of the PEM fuel cell unit from Fig. 1 are schematically represented in detail in Fig. 2, were: 1 – gas inlet tube, 2 – gas outlet tube, 3 – end plate, 4 – sealing gasket, 5 – current collector, 6 – graphite bipolar plate, 7- Teflon gasket, 8 – Membrane Electrode Assembly(MEA), 9 – fastening screws. Operational parameters like temperature, flow rate, relative humidity of the supplied gases, stoichiometry along with current and voltage were recorded and controlled by using a LabVIEW based control and data acquisition system. The reference values have been used for controlling the fuel cell and reactant temperatures, "dew point" temperature (for 80% relative humidity) and anodic/cathodic inlet pressures in the present experiments.

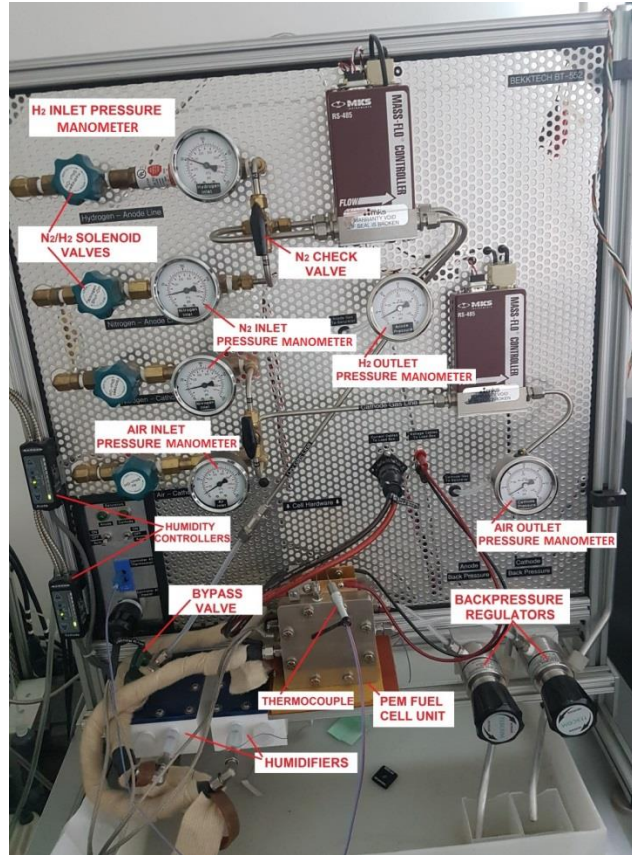


Fig. 3 BEKKTECH BT-552 PEM fuel cell station used in experiments

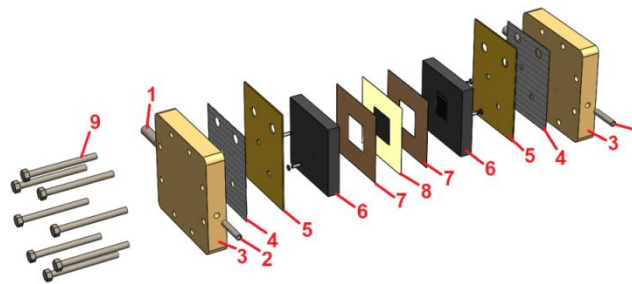


Fig. 4 Schematic representation of the PEM unit cell used in the BEKKTECH BT-552 testing system, with all components included.

Figure 4 shows the anodic bipolar graphite plates used in the PEM fuel assembly, with a specific flow pattern based on single channels arranged in the form of a serpentine. The flow fields were created on graphite plates by milling using a Computer Numerical Control (CNC) machine from the research laboratory 3NANO-SAE Research Center Bucharest. DURA-slate ST100 bipolar plates manufactured by Sainergy Tech USA with porosity under 1, graphite volume density of 2g/cm^3 , null gas permeability and electrical conductivity over 300 S/cm have been processed here.

For both types of measurements, two different backpressure values were considered at the anode and cathode of the fuel cell, as can be seen in Table 4, where reference gas pressure pressures at the system entry are shown ($P_{\text{ref,a}}$, $P_{\text{ref,c}}$), as well as the volumetric flow rates at anode and cathode ($q_{\text{ref,a}}$ and $q_{\text{ref,c}}$).

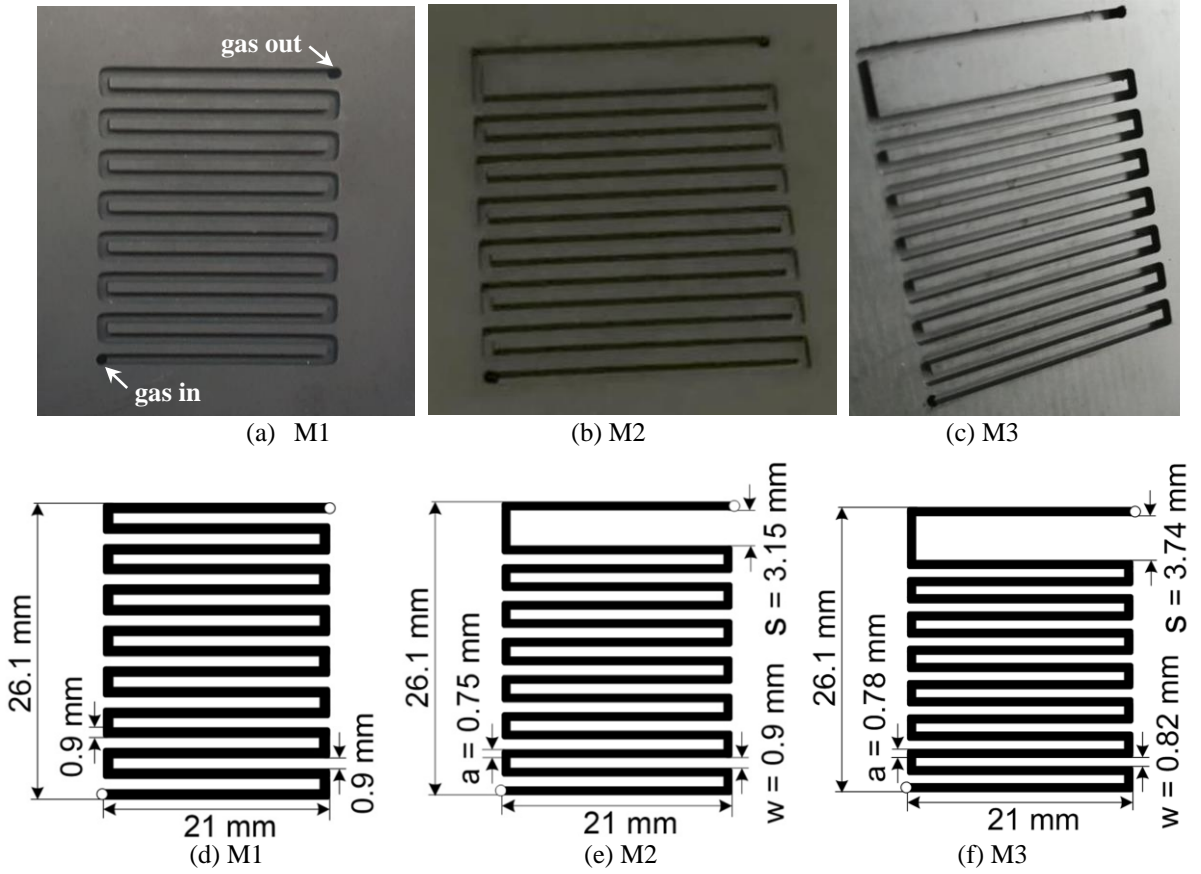


Fig. 3 (a) - (c) Images of the bipolar graphite plates used at anode and (d) - (f) geometric dimensions of the serpentine shaped channel fields for the M1, M2 and M3 models

Table 4 Reference values for pressure and flow rates for the two types of experimental measurements

Experimental tests	$q_{ref,a}$ (sccm)	$q_{ref,c}$ (sccm)	$P_{ref,a}$ (kPa)	$P_{ref,c}$ (kPa)	$P_{b,a}$ (kPa)	$P_{b,c}$ (kPa)
Flow field optimization	150	600	300	200	30;70	30;70
MEA assembly influence on fuel cell efficiency	200	800	400	150	20;50	30;70

In fig. 4 are presented the experimental polarization curves for models M1-M3 at two different backpressures, obtained along the Experiment no.1(Flow field optimization). As we can see in Fig. 4.a, at a backpressure of 30 kPa, the fuel cell having the bipolar flow field M2 entered rapidly in the concentration loss region, starting with a current density of only 0.7 A/cm². We could observe also here that at current densities over 0.75 A/cm², the fuel cell polarization curves for flow fields M1 and M3 are close to each other, due to similar ohmic losses. From Fig. 4.b we noticed almost identical performances of the cell at low current densities (under 0.4 A/cm²) for the flow fields M1 and M2, indicating similar activation losses.

From Fig. 4.b we can notice a reduction in the slope of the polarization curve for the M3 field model compared to the other two models at the backpressure of 70 kPa, thus indicating better performance of the bipolar plate with a w/a ratio (land to channel ratio) equal to 1.05. This

behavior can be associated with achieving the best compromise between the advantages and disadvantages of using a flow field with $w/a > 1$, as mentioned in the literature.

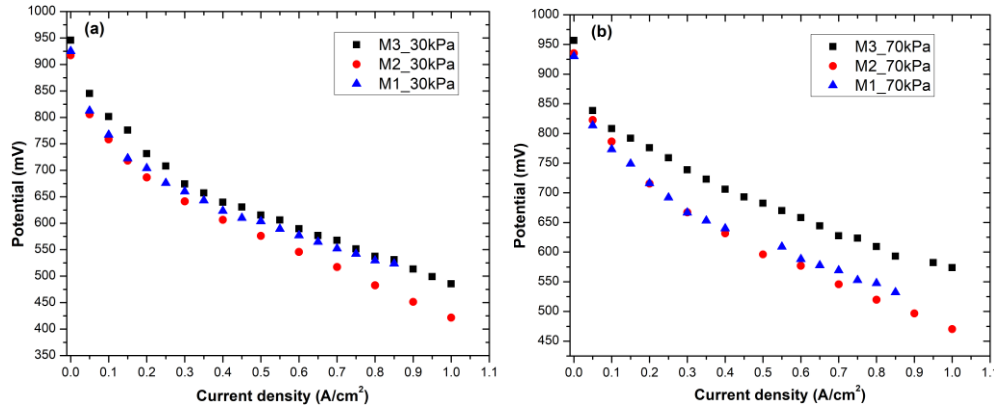


Fig. 4 Experimental polarization curves for the PEMF fuel cell with three different fields for the flow channels, obtained at two backpressures(Experiment no.1)

In fig. 5 was plotted the energetic (thermodynamic) efficiency determined on the basis of the relationship (3) for the two experimental tests of the PEMFC system, with different types of bipolar plate flow fields. In the case of model M2 with the highest w/a ratio of 1.2 was observed a rapid exponential decrease of the thermodynamic efficiency starting from a power density of 0.25 W/cm^2 , from 0.48 to 0.33 at a backpressure of 30 kPa (see fig. 5.a).

Model M3 presented a linear variation of energetic efficiency along the entire power density domain at backpressure of 70 kPa, with values increased by 7 – 14% at power densities between $0.115 - 0.44 \text{ W/cm}^2$ by comparing with model M2, as we could notice in fig. 5.b.

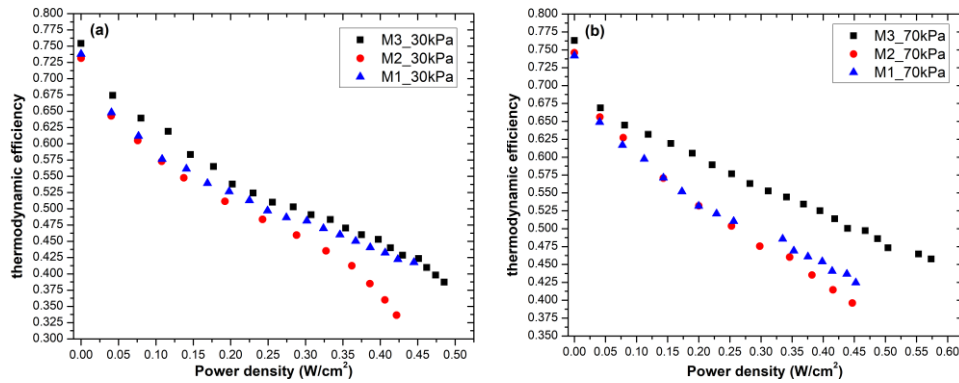


Fig. 5 Experimental variation of thermodynamic efficiency at various values of power density for the PEMFC system (experiment no. 1)

By comparing the evolution of exergy along the current density from one flow field model to another at a backpressure of 30 kPa (see fig. 6.a), we could observe that at current densities over 0.75 A/cm^2 , the exergy efficiency curves for flow fields M1 and M3 are close to each other, due to a similar electrical power W_{net} generated at high current densities in this case (deviations of only 1.3 – 2 %) for the two models.

At the backpressure of 70 kPa(see fig. 6.b), exergy efficiency for model M3 had values modifying from 53.3 % to 34.1 % , obtained while the current density changed from 0.05 to 1 A/cm^2 . An efficiency enhancement, starting from a value of 3.9 % at 0.05 A/cm^2 and at a net

power of 0.23 W till 11.4 -17.5 % at 0.8 A/cm² and 2.66 W was registered for this model, by comparing with models M1 and M2, respectively.

As we can see in fig. 7, thermodynamic irreversibility of the PEMFC system increased by increasing the current density, due to the decreasing of the ratio between the performed work and input energy of the cell. From fig. 7.a. we could observe that models M1 and M3 had similar irreversibility's, but lower with about 4.2 % at 0.4 A/cm² and 5.1 % at 0.8 A/cm² than the model M2.

In fig. 7.b. we could notice a clear reduction of irreversibility for model M3 by comparing with the other two models along the entire current density domain, with a value of 0.866 W at 0.2 A/cm² and 5.78 W at 1 A/cm². At the beginning of the high current density domain considered here (0.7 A/cm²), irreversibility's for model M3 decreased with 10% by reporting with model M2 and with 7.1% after comparing with model M1.

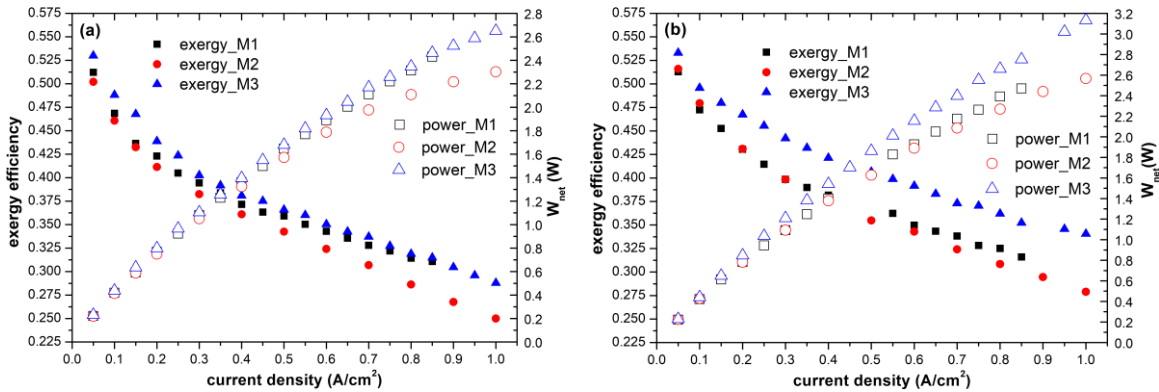


Fig. 6. Exergy efficiency and generated electrical power variations for PEMFC cell with flow field models M1-M3 at two different system backpressures: a) 30kPa and b) 70kPa(Experiment no.1)

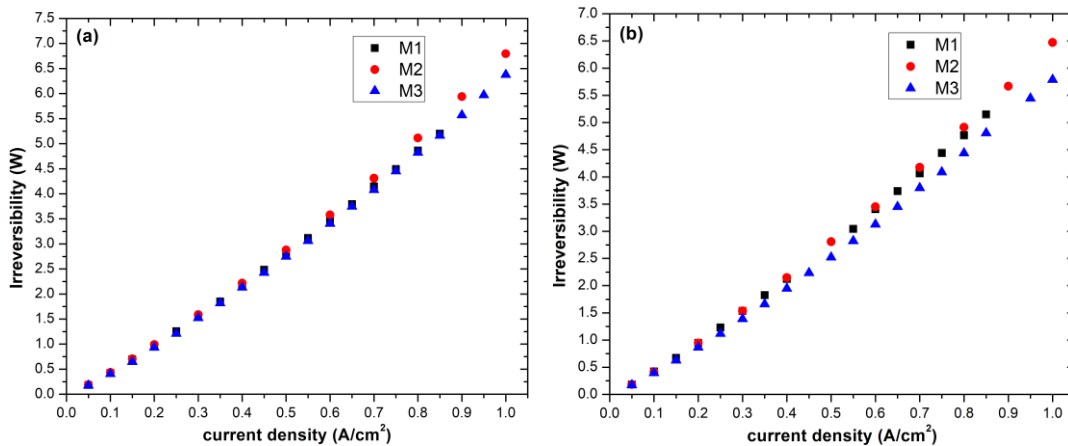


Fig. 7. Thermodynamic irreversibility evolution at different current density steps for the fuel cell with flow field models M1-M3 at two different system backpressures: a) 30kPa and b) 70kPa(Experiment no.1)

7. SUMMARY OF CHAPTER 7

Using a semi-empirical mathematical model that takes into account the voltage loss through activation, the ohmic losses and the concentration losses according to the operating temperature, the partial pressures of the reactants and the properties of the protonic membrane (thickness, humidity, conductivity) could reasonably estimate the variation of the cell voltage in relation to the current density for the fuel cell. Fuel cell contained the M3 optimized flow field and the

Nafion 117 PEM membrane based MEA assembly and worked under normal $P_{b,a}/P_{b,c} = 20/30$ kPa along the Experiment no. 2.

At the backpressure of 30kPa , with H_2 and O_2 partial pressures of 145.8 kPa and 20.1 kPa, respectively inside the combustion cell (Experiment no. 1), the M3 flow pattern with $w/a = 1.05$ showed the polarization curve with the lowest activation losses and ohmic losses up to a current density of 0.75 A/cm^2 . After this value, at high current densities, the ohmic losses for the M3 and M1 models ($w/a = 1$) have become very close. At the backpressure of 70 kPa, with partial pressures of 165.8 kPa for H_2 and 24.3 kPa for O_2 along the cell, a significant reduction in the slope of the polarization curve for the M3 model was observed, thus suggesting an improved electrical performance of the fuel cell with this model of the flow field created on his bipolar plates.

CONCLUSIONS

At a system backpressure of 30 kPa, with partial pressures of 145.8 kPa for H_2 and 20.1 kPa for O_2 inside the PEM fuel cell, the flow field M3 with ratio $w/a = 1.05$ presented the polarization curve with lowest activation and ohmic losses till at a current density of 0.75 A/cm^2 . After this value, at high current densities, the ohmic losses for the models M3 and M1 (with w/a ratio of 1) seemed to be similar.

At a backpressure of 70 kPa, with partial pressures of 165.8 kPa for H_2 and 24.3 kPa for O_2 through the cell, a big slope reduction for polarization curve of the model M3 was observed, suggesting a much better electrical performance of the fuel cell with this type of the gas flow field along the entire current density domain.

The power density curves for the cell with flow fields M1 and M3 proved to be near to each other at a backpressure of 30 kPa, but at a higher backpressure a clear enhancement of 10 – 11% was observed for model M1 at current densities over 0.7 A/cm^2 .

Optimized model M3 presented the highest thermodynamic efficiency along the entire power density domain for both pressure conditions considered in the experimental testing.

Increasing backpressure of the PEM fuel cell system from 30 kPa to 70 kPa, the exergy efficiency increased and thermodynamic irreversibility decreased as a consequence of reduced irreversible losses at anode and cathode which enhanced the performance of the fuel cell.

The fuel cell with optimized bipolar plate flow field model M3, having channel width/rib width dimensions of 0.78/0.82 mm, presented at a current density of 0.85 A/cm^2 and at a net power of 2.75 W an exergy efficiency enhancement of 11.4 % by comparing with model M1 and 17.5 % after comparing with model M2, with an equivalent reduction of thermodynamic irreversibility of 7.1% and 10%, respectively, at a current density of 0.7 A/cm^2 .

Irreversibility rate minimization and enhancement of the exergy efficiency of the PEM fuel cell offer the possibility of cost reduction for the energetic system by lowering the number of cells in the PEMFC stack, for example, and bipolar plate flow field optimization can be an important factor for enhanced commercialization of the PEM fuel cell stacks.